



RESEARCH ARTICLE

Potentiometric and Thermodynamic Studies of Some Schiff-base Derivatives of 4-Aminoantipyrine and Their Metal Complexes

A.A. El-Bindary¹, A.Z. El-Sonbati¹, M.A. Diab¹, E.E. El-Katori² and H.A. Seyam¹

1.Department of Chemistry, Faculty of Science, Damietta University, Damietta 34517, Egypt.

2.Department of Chemistry, Faculty of Science, King Khalid University, Abha, KSA.

Manuscript Info

Manuscript History:

Received: 13 February 2014
Final Accepted: 22 March 2014
Published Online: April 2014

Key words:

Antipyrine, Geometrical structure, Potentiometry and thermodynamic.

*Corresponding Author

A.A. El-Bindary

Abstract

4-(4-hydroxybenzalidineamine) antipyrine (L_1) and 4-(2-hydroxybenzalidineamine) antipyrine (L_2) have been synthesized and their structure have been confirmed by elemental analyses, mass spectrometry, IR and ^1H NMR spectroscopy. The geometrical structures of these ligands are carried out by HF method with 3-21G basis set. The proton-ligand dissociation constant of the ligands (L_1 and L_2) and metal-ligand stability constants of their complexes with metal ions (Mn^{2+} , Co^{2+} , Ni^{2+} and Cu^{2+}) have been determined potentiometrically in 0.1 mol.dm⁻³ KCl and 10 % (by volume) ethanol–water mixture. The stability constants of the formed complexes increases in the order Mn^{2+} , Co^{2+} , Ni^{2+} and Cu^{2+} . The effect of temperature was studied at 298, 308 and 318 K and the corresponding thermodynamic parameters (ΔG , ΔH and ΔS) were derived and discussed. The dissociation process is non-spontaneous, endothermic and entropically unfavorable. The formation of the metal complexes has been found to be spontaneous, endothermic and entropically favorable.

Copy Right, IJAR, 2014., All rights reserved.

1. Introduction

Schiff bases form an interesting class of chelating ligands that has enjoyed popular use in the coordination chemistry of transition and inner transition metals which show various industrial, biological and catalytic applications [1], due to its greater choice, sensitivity and synthetic flexibility to coordination with different transition metal ions [2-5]. Various studies have shown that, the azomethine group ($>\text{C}=\text{N}-$) in Schiff base metal complexes has considerable biological significance and found to be responsible for biological activity such as fungicidal and insecticidal [6]. Schiff bases of 4-aminoantipyrine and its complexes are known for their variety of applications in the area of catalysis [7], clinical applications [8], and pharmacology [9]. Also, antipyrines have found applications outside the pharmaceutical field, such as in the solvent extraction of metal ions [10] and as ligands in complexes with catalytic activity [11]. In continuation of our previous work [12-16], the present work is centered on the synthesis and characterization of two Schiff bases derived from the condensation of 4-hydroxybenzaldehyde/2-hydroxybenzaldehyde with 4-aminoantipyrine. In addition, the geometrical structure of the ligands L_1 and L_2 by HF method with 3-21G basis set was studied. The dissociation constant of the ligands (L_1 and L_2) and the stability constants of their complexes with Mn^{2+} , Co^{2+} , Ni^{2+} and Cu^{2+} at different temperatures are also studied. Furthermore, the corresponding thermodynamic functions are evaluated and discussed.

2. Experimental

2.1. Measurements

All the compounds and solvents used were purchased from Alderich or Sigma. C, H and N were determined on Perkin-Elmer (2400) CHNS analyzer. Spectroscopic data were obtained using the following instruments: FT-IR spectra (KBr discs, 4000-400 cm^{-1}) by Jasco-4100 spectrophotometer; the ^1H NMR spectra by Bruker WP 300 MHz using DMSO-d_6 as a solvent containing TMS as the internal standard; Mass spectra by Shimadzu Qp-2010 Plus. The pH measurements were performed with a Metrohm 836 Titrando (KF & Potentiometric Titrator) equipped with a combined porolyte electrode. The pH-meter readings in the non-aqueous medium were corrected [17]. The electrode system was calibrated according to the method of Irving et al. [18]. Titrations were performed in a double walled glass cell in an inert atmosphere (nitrogen) at ionic strength of 0.1 M KCl. Potentiometric measurements were carried out at different temperature. The temperature was controlled to within ± 0.05 K by circulating thermostated water (Neslab 2 RTE 220) through the outer jacket of the vessel.

The molecular structures of the investigated compounds were optimized by HF method with 3-21G basis set. The molecules were built with the Perkin Elmer ChemBio Draw and optimized using Perkin Elmer ChemBio 3D software. Quantum chemical parameters such as the highest occupied molecular orbital energy (E_{HOMO}), the lowest unoccupied molecular orbital energy (E_{LUMO}) and HOMO-LUMO energy gap (ΔE) for the investigated molecules are calculated.

2.2. Synthesis of the ligands

The Schiff bases (L_1 and L_2 , Fig. 1) have been prepared according to the previous procedure [19]. An ethanolic solution of 4-aminoantipyrine (0.1 mmol) was added slowly to the solution of 4-hydroxybenzaldehyde/2-hydroxybenzaldehyde (0.1 mmol) in ethanol with constant stirring. The mixture was refluxed for 2 hr in a water bath. After concentration of the solution, the precipitate was separated, filtered, washed with ethanol and dried in vacuum over anhydrous CaCl_2 .

4-(4-hydroxybenzalideneamine) antipyrine (L_1). Yield 80 %, Yellow solid, m.p. 228-230 $^\circ\text{C}$. Anal. Calc. for $\text{C}_{18}\text{H}_{17}\text{N}_3\text{O}_2$ (M=307): C, 70.35; H, 5.53; N, 13.68. Found: C, 70.05; H, 5.43; N, 13.58. MS m/z 307 (M^+). FT-IR (cm^{-1} , KBr discs): 3180m, $\nu_{\text{O-H}}$; 1655s, $\nu_{\text{C=O}}$; 1581m, $\nu_{\text{C=N}}$; 1371m, $\nu_{\text{C-N}}$. ^1H NMR (ppm): 10.12 (s, 1H, OH); 8.32 (s, 1H, CH=N).

4-(2-hydroxybenzalideneamine)antipyrine (L_2). Yield 82 %, Pale-yellow solid, m.p. 198-200 $^\circ\text{C}$. Anal. Calc. for $\text{C}_{18}\text{H}_{17}\text{N}_3\text{O}_2$ (M=307): C, 70.35; H, 5.53; N, 13.68. Found: C, 69.95; H, 5.35; N, 13.45. MS m/z 307 (M^+). FT-IR (cm^{-1} , KBr discs): 3190m, $\nu_{\text{O-H}}$; 1648s, $\nu_{\text{C=O}}$; 1589m, $\nu_{\text{C=N}}$; 1351m, $\nu_{\text{C-N}}$. ^1H NMR (ppm): 10.12 (s, 1H, OH); 8.32 (s, 1H, CH=N).

2.3. Potentiometric studies.

A ligand solution ($0.001 \text{ mol.dm}^{-3}$) was prepared by dissolving an accurately weighted amount of the solid in ethanol (AnalaR). Metal ion solutions ($0.0001 \text{ mol.dm}^{-3}$) were prepared from AnalaR metal chlorides in bidistilled water and standardized with EDTA [20]. Solutions of $0.001 \text{ mol.dm}^{-3}$ HCl and 1 mol.dm^{-3} KCl were also prepared in bidistilled water. A carbonate-free sodium hydroxide solution in 10% (by volume) ethanol-water mixture was used as titrant and standardized against oxalic acid (AnalaR).

The apparatus, general conditions and methods of calculation were the same as in previous work [14-16]. The following mixtures (i) – (iii) were prepared and titrated potentiometrically at 298 K against standard $0.002 \text{ mol.dm}^{-3}$ NaOH in a 10 % (by volume) ethanol-water mixture:

i) 5 cm^3 $0.001 \text{ mol.dm}^{-3}$ HCl + 5 cm^3 1 mol.dm^{-3} KCl + 5 cm^3 ethanol.

ii) 5 cm^3 $0.001 \text{ mol.dm}^{-3}$ HCl + 5 cm^3 1 mol.dm^{-3} KCl + 5 cm^3 $0.001 \text{ mol.dm}^{-3}$ ligand.

iii) 5 cm^3 $0.001 \text{ mol.dm}^{-3}$ HCl + 5 cm^3 1 mol.dm^{-3} KCl + 5 cm^3 $0.001 \text{ mol.dm}^{-3}$ ligand + 10 cm^3 $0.0001 \text{ mol.dm}^{-3}$ metal chloride.

For each mixture, the volume was made up to 50 cm^3 with bidistilled water before the titration. These titrations were repeated for temperatures of 308 and 318 K. All titrations have been carried out between pH 3.0 – 11.0 and under nitrogen atmosphere.

3. Results and Discussion

3.1. Molecular Structure

The selected geometrical structures of the investigated ligands are calculated by optimizing their bond lengths and bond angles. The calculated molecular structures for L_1 and L_2 are shown in Fig. 2. The selected geometric parameters are listed in Table 1. The C10-N8 bond with length 1.26 Å for both ligands is

a normal imine bond. The phenyl and pyrazoline rings form a nearly planar dihedral angle (179.56°), and the pyrazoline and directly linked benzene form an effective dihedral angle (132.76°) for both ligands. From Table 2 the computed net charges on active centers, it is found that the most negative centers in L₁ and L₂ are N4 and O17. The surfaces of frontier molecular orbital theory (FMOs) are shown in Fig. 3.

The HOMO–LUMO energy gap, ΔE, which is an important stability index, is applied to develop theoretical models for explaining the structure and conformation barriers in many molecular systems. The smaller is the value of ΔE, the more is the reactivity of the compound has [21-24]. The first derivative of the energy with respect to an applied electric field, is used to discuss and rationalize the structure [25,26]. The calculated quantum chemical parameters are given in Table 3. The ligand L₂ is more reactive than L₁ as reflected from energy gap values Table 3. Additional parameters such as ΔE, absolute Electronegativities, χ, chemical potentials, Pi, absolute hardness, η, absolute softness, σ, global electrophilicity, ω, [27-29] global softness, S, and additional electronic charge, ΔN_{max}, have been calculated according to the following equations [30]:

$$\Delta E = E_{LUMO} - E_{HOMO} \quad (1)$$

$$\chi = \frac{-(E_{HOMO} + E_{LUMO})}{2} \quad (2)$$

$$\eta = \frac{E_{LUMO} - E_{HOMO}}{2} \quad (3)$$

$$\sigma = 1/\eta \quad (4)$$

$$Pi = -\chi \quad (5)$$

$$S = \frac{1}{2\eta} \quad (6)$$

$$\omega = Pi^2 / 2\eta \quad (7)$$

$$\Delta N_{max} = -Pi / \eta \quad (8)$$

3.2. Potentiometric measurements

The average number of the protons associated with the ligands (L₁ and L₂) at different pH values, \bar{n}_A , was calculated from the titration curves of the acid in the absence and presence of L₁ and L₂. Applying eq. 9:

$$\bar{n}_A = Y \pm \frac{(V_1 - V_2)(N^o + E^o)}{(V^o - V_1)TC_L^o} \quad (9)$$

where Y is the number of available protons in L₁ and L₂ (Y=1) and V₁ and V₂ are the volumes of alkali required to reach the same pH on the titration curve of hydrochloric acid and reagent, respectively, V^o is the initial volume (50 cm³) of the mixture, TC_L^o is the total concentration of the reagent, N^o is the normality of sodium hydroxide solution and E^o is the initial concentration of the free acid. Thus, the formation curves (\bar{n}_A vs. pH) for the proton-ligand systems were constructed and found to extend between 0 and 1 in the \bar{n}_A scale. This means that L₁ and L₂ has one ionizable proton (the enolized hydrogen ion of the hydroxyl group, pK^H). Different computational methods [31] were applied to evaluate the dissociation constant. Three replicate titrations were performed; the average values obtained are listed in Table 4. The completely protonated form of the ligands L₁ and L₂ has one dissociable proton, that dissociates in the measurable pH range. The deprotonation of the o-hydroxy group (ligand L₂) most probably results in the formation of stable intramolecular H-bonding with the nitrogen atom of the C=N group. Such an interaction decreases the dissociation process of ligand L₂, i.e. increases the pK^H value [32,33].

The formation curves for the metal complexes were obtained by plotting the average number of ligands attached per metal ion (\bar{n}) vs. the free ligand exponent (pL), according to Irving and Rossotti [34]. The average number of the reagent molecules attached per metal ion, \bar{n} , and free ligand exponent, pL, can be calculated using eqs 10 and 11:

$$\bar{n} = Y \pm \frac{(V_3 - V_2)(N^o + E^o)}{(V^o - V_2).\bar{n}_A.TC_M^o} \quad (10)$$

and

$$pL = \log_{10} \frac{\sum_{n=0}^{n=J} \beta_n^H \left(\frac{1}{[H^+]} \right)^n}{TC_L^o - \bar{n} TC_M^o} \cdot \frac{V^o + V_3}{V^o} \quad (11)$$

where TC_M^o is the total concentration of the metal ion present in the solution, β_n^H is the overall proton-reagent stability constant. V_1 , V_2 and V_3 are the volumes of alkali required to reach the same pH on the titration curves of hydrochloric acid, organic ligand and complex, respectively. These curves were analyzed and the successive metal-ligand stability constants were determined using different computational methods [35,36]. The values of the stability constants ($\log K_1$ and $\log K_2$) are given in Table 5. The following general remarks can be pointed out:

(i) The maximum value of \bar{n} was ~ 2 indicating the formation of 1:1 and 1:2 (metal : ligand) complexes only [37].

(ii) The metal ion solution used in the present study was very dilute (2×10^{-5} mol dm⁻³), hence there was no possibility of formation of polynuclear complexes [38,39].

(iii) The metal titration curves were displaced to the right-hand side of the ligand titration curves along the volume axis, indicating proton release upon complex formation of the metal ion with the ligand. The large decrease in pH for the metal titration curves relative to ligand titration curves point to the formation of strong metal complexes [40,41].

(iv) For the same ligand at constant temperature, the stability of the chelates increases in the order Mn²⁺, Co²⁺, Ni²⁺ and Cu²⁺ [42-44]. This order largely reflects that the stability of Cu²⁺ complexes are considerably larger than those of other metals of the 3d series. Under the influence of both the polarizing ability of the metal ion [45] and the ligand field [45] Cu²⁺ will receive some extra stabilization due to tetragonal distortion of octahedral symmetry in its complexes. The greater stability of Cu²⁺ complexes is produced by the well known *Jahn-Teller* effect [46].

The dissociation constant (pK^H) for L₁ and L₂, as well as the stability constants of its complexes with Mn²⁺, Co²⁺, Ni²⁺ and Cu²⁺ have been evaluated at 298, 308, and 318 K, and are given in Tables 4 and 5, respectively. The enthalpy (ΔH) for the dissociation and complexation process was calculated from the slope of the plot pK^H or $\log K$ vs. $1/T$ using the graphical representation of *van't Hoff* eqs. 12 and 13:

$$\Delta G = -2.303 RT \log K = \Delta H - T \Delta S \quad (12)$$

or

$$\log K = (-\Delta H / 2.303 R)(1/T) + (\Delta S / 2.303 R) \quad (13)$$

From the ΔG and ΔH values one can deduce the entropy ΔS using the well known relationships 12 and 14:

$$\Delta S = (\Delta H - \Delta G) / T \quad (14)$$

All thermodynamic parameters of the dissociation process of L₁ and L₂ are recorded in Table 4. From these results the following conclusions can be made:

(i) The pK^H values decrease with increasing temperature, i.e. the acidity of the ligand increases [16].

(ii) A positive value of ΔH indicates that dissociation is accompanied by absorption of heat and the process is endothermic [47].

(iii) A positive value of ΔG indicates that the dissociation process is not spontaneous [48].

(iv) A negative value of ΔS is obtained due to the increased order as a result of the solvation process.

All the thermodynamic parameters of the stepwise stability constants of complexes are recorded in Tables 6 and 7. It is known that the divalent metal ions exist in solution as octahedrally hydrated species [36] and the obtained values of ΔH and ΔS can then be considered as the sum of two contributions: (a) release of H₂O molecules, and (b) metal-ligand bond formation. Examination of these values shows that:

(i) The stability constants ($\log K_1$ and $\log K_2$) for L₁ and L₂ complexes decrease with increasing temperature [49].

(ii) The negative value of ΔG for the complexation process suggests the spontaneous nature of such processes.

(iii) The ΔH values are positive, meaning that these processes are endothermic and favorable at higher temperature.

(iv) The ΔS values for the complexes are positive, confirming that the complex formation is entropically favorable [14].

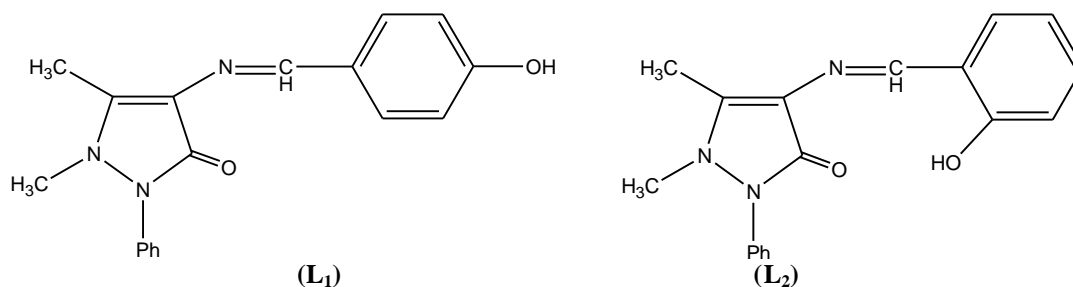


Fig. 1. Structure of the ligands L₁ and L₂.

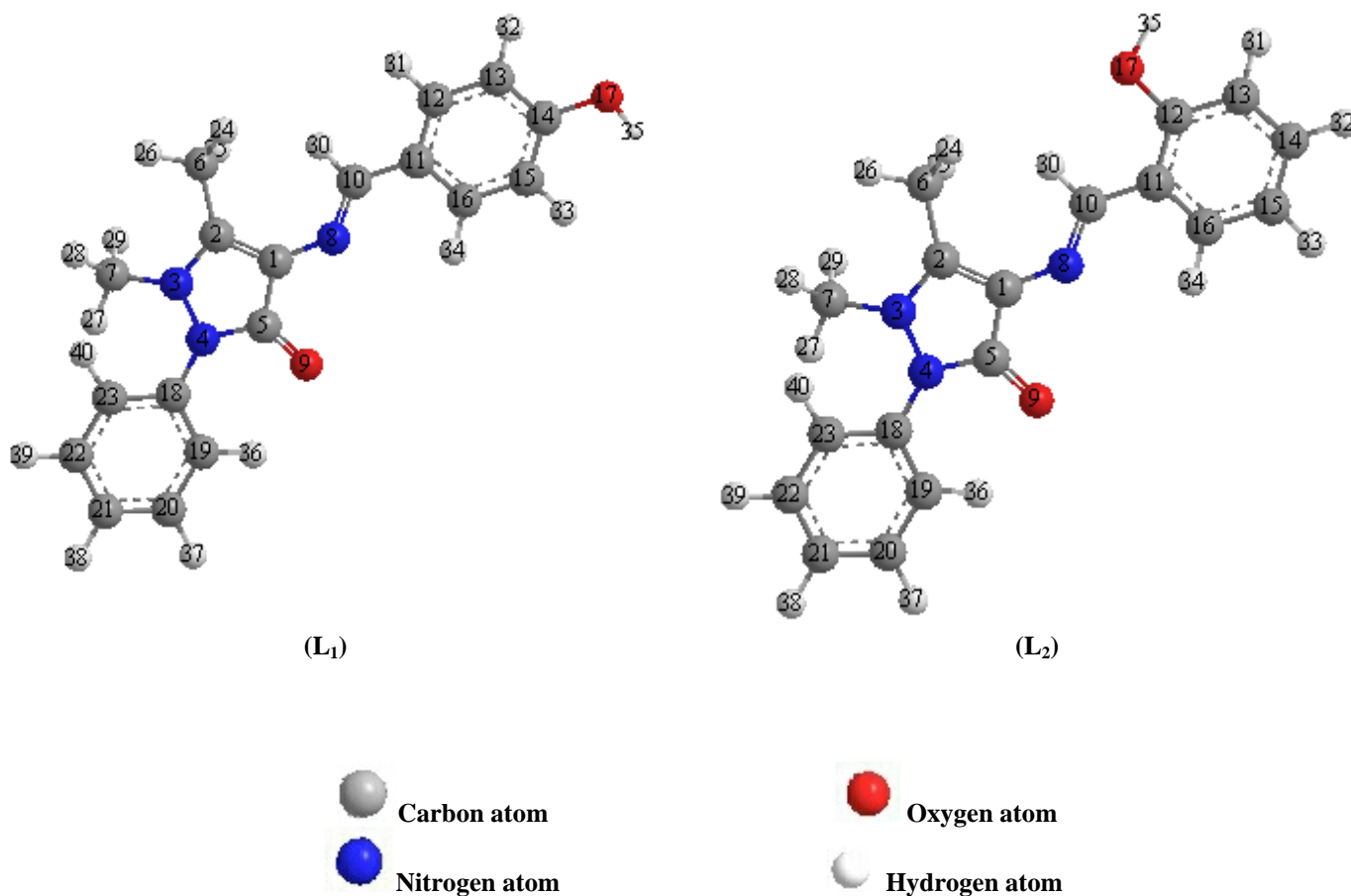


Fig. 2. Molecular structure with atomic numbering for L₁ and L₂.

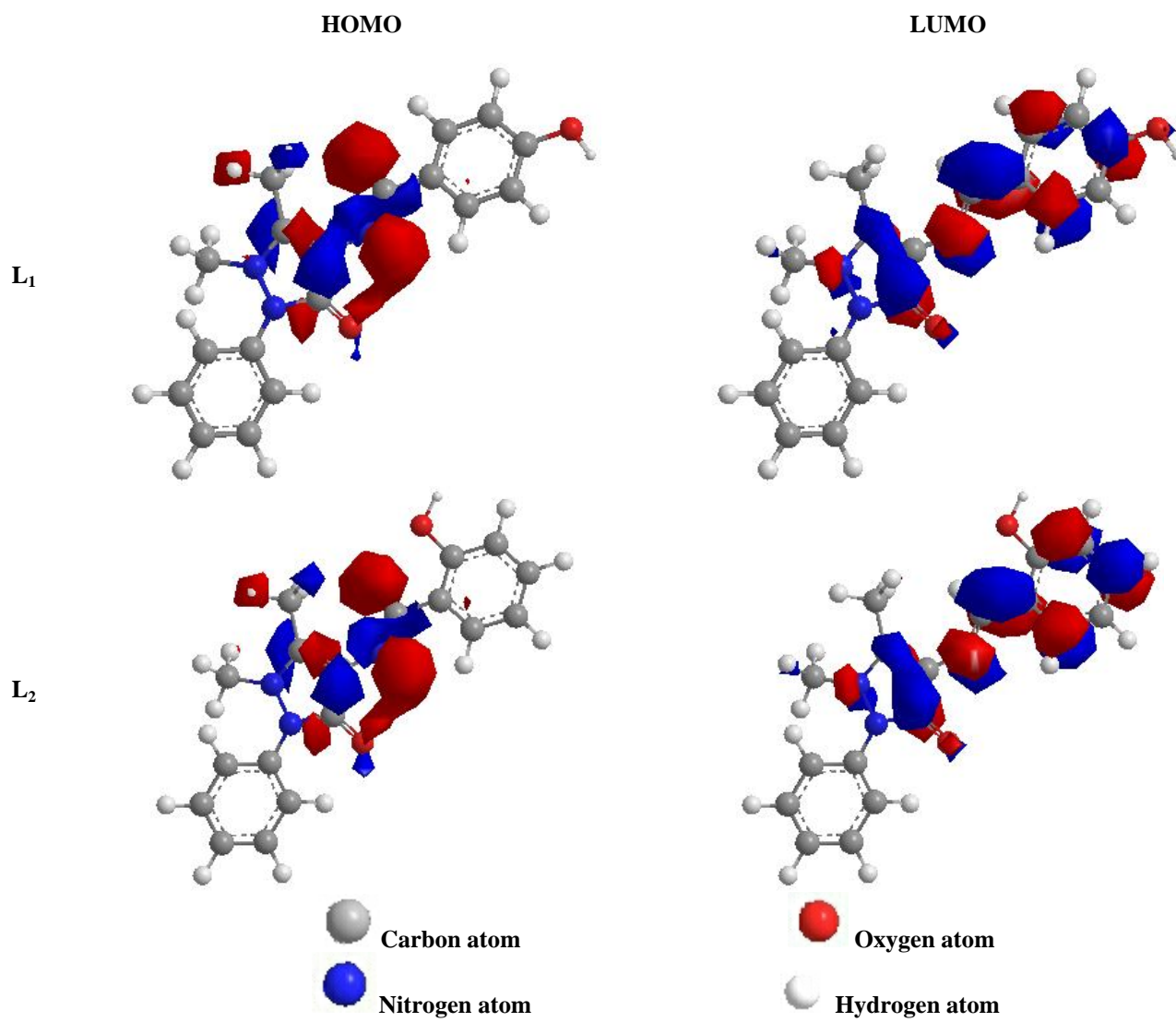


Fig. 3. Surface of FMOs for L₁ and L₂.

Table 1. The selected geometric parameters for L₁ and L₂.

L ₁				L ₂			
Bond lengths (Å)		Bond angles (°)		Bond lengths (Å)		Bond angles (°)	
C11-C16	1.347	C23-C22-C21	120.038	C11-C16	1.348	C23-C22-C21	120.037
C15-C16	1.342	C22-C21-C20	118.996	C15-C16	1.341	C22-C21-C20	118.995
C14-C15	1.343	C21-C20-C19	120.314	C14-C15	1.339	C21-C20-C19	120.316
C13-C14	1.343	C18-C23-C22	122.266	C13-C14	1.34	C18-C23-C22	122.27
C12-C13	1.342	C20-C19-C18	121.956	C12-C13	1.345	C20-C19-C18	121.955
C11-C12	1.347	C23-C18-C19	116.42	C11-C12	1.353	C23-C18-C19	116.417
C18-C23	1.349	C23-C18-N4	119.472	C18-C23	1.349	C23-C18-N4	119.454
C22-C23	1.342	C19-C18-N4	124.092	C22-C23	1.342	C19-C18-N4	124.113
C21-C22	1.34	C5-N4-N3	102.383	C21-C22	1.34	C5-N4-N3	102.371
C20-C21	1.34	C5-N4-C18	130.41	C20-C21	1.34	C5-N4-C18	130.451
C19-C20	1.343	N3-N4-C18	122.965	C19-C20	1.343	N3-N4-C18	122.966
C18-C19	1.349	C16-C15-C14	121.512	C18-C19	1.349	C16-C15-C14	119.613
N3-C2	1.277	C15-C14-C13	117.34	N3-C2	1.277	C15-C14-C13	119.165
C1-C2	1.348	C15-C14-O17	120.997	C1-C2	1.348	C14-C13-C12	121.867
C5-C1	1.367	C13-C14-O17	121.663	C5-C1	1.367	C11-C16-C15	121.53
N4-C5	1.274	C14-C13-C12	121.417	N4-C5	1.274	C13-C12-C11	118.976
N3-N4	1.362	C11-C16-C15	121.165	N3-N4	1.362	C13-C12-O17	118.616
C14-O17	1.36	C13-C12-C11	121.256	C12-O17	1.363	C11-C12-O17	122.409
C10-C11	1.349	C16-C11-C12	117.311	C10-C11	1.351	C16-C11-C12	118.849
N8-C10	1.265	C16-C11-C10	122.293	N8-C10	1.265	C16-C11-C10	120.83
C5-O9	1.216	C12-C11-C10	120.396	C5-O9	1.216	C12-C11-C10	120.321
C1-N8	1.267	C11-C10-N8	124.732	C1-N8	1.268	C11-C10-N8	125.13
N4-C18	1.279	C10-N8-C1	128.716	N4-C18	1.279	C10-N8-C1	128.653
N3-C7	1.485	C1-C5-N4	111.35	N3-C7	1.485	C1-C5-N4	111.354
C2-C6	1.509	C1-C5-O9	124.14	C2-C6	1.509	C1-C5-O9	124.178
		N4-C5-O9	124.366			N4-C5-O9	124.323
		C2-N3-N4	114.198			C2-N3-N4	114.205
		C2-N3-C7	116.13			C2-N3-C7	116.114
		N4-N3-C7	129.113			N4-N3-C7	129.113
		N3-C2-C1	104.508			N3-C2-C1	104.495
		N3-C2-C6	127.735			N3-C2-C6	127.677
		C1-C2-C6	127.535			C1-C2-C6	127.605
		C2-C1-C5	106.36			C2-C1-C5	106.353
		C2-C1-N8	134.216			C2-C1-N8	134.251
		C5-C1-N8	119.417			C5-C1-N8	119.389

Table 2. Net charges on active centers of the studied ligands (L₁ and L₂).

Atom	Charges	
	L ₁	L ₂
N3	-0.4891	-0.4891
N4	-0.157	-0.157
N8	-0.621	-0.621
O9	-0.57	-0.57
O17	-0.5325	-0.5325

Table 3. The calculated quantum chemical parameters for L₁ and L₂.

Ligand	HOMO (a.u)	LUMO (a.u)	ΔE (a.u)	X (a.u)	η (a.u)	σ (a.u) ⁻¹	Pi (a.u)	S (a.u) ⁻¹	ω (a.u)	ΔN_{\max}
L ₁	-0.2647	-0.0502	0.2146	0.1575	0.1073	9.3205	-0.1575	4.6603	0.1155	1.4675
L ₂	-0.2633	-0.0645	0.1988	0.1639	0.0994	10.0599	-0.1639	5.0299	0.1352	1.6492

Table 4. Thermodynamic functions for the dissociation of ligands (L₁ and L₂) in 10 % (by volume) ethanol–water mixture and 0.1 mol.dm⁻³ KCl at different temperatures.

Ligand	T/K	Dissociation constant	Gibbs energy	Enthalpy	Entropy
		pK ^H	kJ.mol ⁻¹ ΔG_1	kJ.mol ⁻¹ ΔH_1	J.mol ⁻¹ .K ⁻¹ $-\Delta S_1$
L ₁	298	8.00	45.64	28.10	58.86
	308	7.85	46.29		59.05
	318	7.69	46.82		58.86
L ₂	298	9.12	52.03	29.91	74.22
	308	8.96	52.83		74.42
	318	8.79	53.52		74.22

Table 5. Stepwise stability constants for ML and ML₂ complexes of ligands (L₁ and L₂) in 10 % (by volume) ethanol–water mixtures and 0.1 mol.dm⁻³ KCl at different temperatures.

Ligand	M ⁿ⁺	298 K		308 K		318 K	
		log K ₁	log K ₂	log K ₁	log K ₂	log K ₁	log K ₂
L ₁	Mn ²⁺	5.64	4.63	5.79	4.78	5.94	4.94
	Co ²⁺	5.79	4.78	5.95	4.93	6.11	5.08
	Ni ²⁺	5.85	4.83	6.00	4.98	6.16	5.13
	Cu ²⁺	6.14	5.12	6.30	5.28	6.47	5.44
L ₂	Mn ²⁺	7.60	5.80	7.79	5.98	8.00	6.13
	Co ²⁺	7.75	5.88	7.93	6.05	8.04	6.20
	Ni ²⁺	7.81	5.92	7.99	6.18	8.14	6.34
	Cu ²⁺	7.95	6.14	8.15	6.28	8.30	6.44

Table 6. Thermodynamic functions for ML and ML₂ complexes of ligand (L₁) in 10 % (by volume) ethanol–water mixture and 0.1 mol.dm⁻³ KCl.

M ⁿ⁺	T/K	Gibbs energy/kJ.mol ⁻¹		Enthalpy/kJ.mol ⁻¹		Entropy/J.mol ⁻¹ .K ⁻¹	
		$-\Delta G_1$	$-\Delta G_2$	ΔH_1	ΔH_2	ΔS_1	ΔS_2
Mn ²⁺	298	32.18	26.41	27.20	28.10	199.28	182.96
	308	34.14	28.18			199.19	182.77
	318	36.16	30.07			199.29	182.96
Co ²⁺	298	33.03	27.27	29.02	27.20	208.24	182.82
	308	35.08	29.07			208.14	182.73
	318	37.20	30.93			208.25	182.82
Ni ²⁺	298	33.37	27.55	28.10	27.20	206.32	183.78
	308	35.38	29.36			206.13	183.68
	318	37.50	31.23			206.32	183.78
Cu ²⁺	298	35.03	29.21	29.91	29.02	217.96	195.41
	308	37.15	31.13			217.76	195.32
	318	39.39	33.12			217.96	195.42

Table 7. Thermodynamic functions for ML and ML₂ complexes of ligand (L₂) in 10 % (by volume) ethanol–water mixture and 0.1 mol.dm⁻³ KCl.

M ⁿ⁺	T/K	Gibbs energy/kJ.mol ⁻¹		Enthalpy/kJ.mol ⁻¹		Entropy/J.mol ⁻¹ .K ⁻¹	
		-ΔG ₁	-ΔG ₂	ΔH ₁	ΔH ₂	ΔS ₁	ΔS ₂
Mn ²⁺	298	43.36	33.09	33.39	31.63	257.56	217.20
	308	45.94	35.26			257.56	217.20
	318	48.71	37.32			258.17	216.84
Co ²⁺	298	44.22	33.55	31.63	29.87	254.54	212.83
	308	46.76	35.67			254.54	212.83
	318	48.95	37.75			253.41	212.65
Ni ²⁺	298	44.56	33.77	31.63	45.68	255.68	266.65
	308	47.11	36.44			255.68	266.65
	318	49.56	38.60			255.32	265.05
Cu ²⁺	298	45.36	35.03	35.13	24.60	270.12	200.12
	308	48.06	37.03			270.12	200.12
	318	50.13	39.21			269.40	200.67

4. Conclusion

4-(4-hydroxybenzalideneamine) antipyrine and 4-(2-hydroxybenzalideneamine) antipyrine have been synthesized and characterized using spectroscopic techniques. The geometrical structures of these ligands are carried out by HF method with 3-21G basis set. The proton-ligand dissociation constant of the ligands (L₁ and L₂) and metal-ligand stability constants of their complexes with metal ions (Mn²⁺, Co²⁺, Ni²⁺ and Cu²⁺) have been determined potentiometrically in 0.1 mol.dm⁻³ KCl and 10 % (by volume) ethanol–water mixture. The corresponding thermodynamic parameters (ΔG, ΔH and ΔS) were derived and discussed. The dissociation process is non-spontaneous, endothermic and entropically unfavorable. The formation of the metal complexes has been found to be spontaneous, endothermic and entropically favorable.

References

- [1] K. Mohanan, S.N. Devi, B. Murukan, Synth. React. Inorg. Met.-Org. Nan.-Met. Chem. 36 (2006) 441-449.
- [2] C. Spinu, A. Kriza, Acta Chim. Solv. 47 (2000) 179-185.
- [3] S. Baluja, A. Aolanki, N. Kachhadia, J. Iranian Chem. Soc. 3 (2006) 312-317.
- [4] S. Oshima, N. Hirayama, K. Kubono, H. Kousen, T. Honjo, Anal. Sci. 18 (2002) 1351-1355.
- [5] G.G. Mohamed, M.M. Omar, A.M. Hindy, Turkish J. Chem. 30 (2006) 361-379.
- [6] K. Singh, M.S. Barwa, P. Tyagi, Synthesis Eur. J. Med. Chem. 42 (2007) 394-402.
- [7] K. Bernardo, S. Leppard, A. Robert, G. Commenges, F. Dehan, B. Meunier, Inorg. Chem. 35 (1996) 387-396.
- [8] D. Chiamonte, J.M. Steiner, J.D. Broussard, K. Baer, S. Gumminger, E.M. Moeller, D.A. Williams, R. Shumway, Cand. J. Vet. Res. 67 (2003) 183-188.
- [9] T. Hitoshi, N. Tamao, A. Hideyuki, F. Manabu, M. Takayuki, Polyhedron 16 (1997) 3787-3794.
- [10] T. Ito, C. Goto, K. Noguchi, Anal. Chim. Acta 443 (2001) 41-51.
- [11] F. Bao, X. Lu, B. Kang, Q. Wu, Eur. Polym. J. 42 (2006) 928-934.
- [12] F. Borges, C. Guimarães, J.L.F.C. Lima, I. Pinto, S. Reis, Talanta 66 (2005) 670-673.
- [13] A.M. Khedr, A.A. El-Bindary, A.M. Abd El-Gawad, Chem. Pap. 59 (2005) 336-342.
- [14] A.A. El-Bindary, A.Z. El-Sonbati, M.A. Diab, A.M. Barakat, J. Appl. Sol. Chem. Model. 2 (2013) 191-196.
- [15] A.T. Mubarak, A.S. Al-Shihri, H.M. Nassef, A.A. El-Bindary, J. Chem. Eng. Data 55 (2010) 5539-5542.
- [16] A.T. Mubarak, A.A. El-Bindary, J. Chem. Eng. Data 55 (2010) 5543-5546.
- [17] R.G. Bates, M. Paabo, R.A. Robinson, J. Phys. Chem. 67 (1963) 1833-1838.

- [18] H.M. Irving, M.G. Miles, L.D. Pettit, *Anal. Chim. Acta* 38 (1967) 475-488.
- [19] R.M. Issa, A.M. Khedr, H.F. Rizk, *Spectrochim. Acta Part A* 62 (2005) 621-629.
- [20] G.H. Jeffery, J. Bassett, J. Mendham, R.C. Deney, *Vogel's Textbook of Quantitative Chemical Analysis*, 5th Edition. Longman, London (1989).
- [21] T.A. Yousef, G.M. Abu El-Reash, M. Al-Jahdali, El-Bastawesy R. El-Rakhawy, *J. Mol. Struct.* 1053 (2013) 15-21.
- [22] G. Gao, C. Liang, *Electrochim. Acta* 52 (2007) 4554-4559.
- [23] Y. Feng, S. Chen, W. Guo, Y. Zhang, G. Liu, *J. Electroanal. Chem.* 602 (2007) 115-122.
- [24] A.Z. El-Sonbati, M.A. Diab, A.A. El-Bindary, Sh.M. Morgan, *Spectrochim. Acta A* 127 (2014) 310-328.
- [25] G. Gece, S. Bilgiç, *Corros. Sci.* 51 (2009) 1876-1878.
- [26] N.A. El-Ghamaz, A.Z. El-Sonbati, M.A. Diab, A.A. El-Bindary, M.K. Awad, Sh.M. Morgan, *Mater. Sci. Semicond. Process.* 19 (2014) 150-162.
- [27] R.G. Pearson, *J. Org. Chem.* 54 (1989) 1423-1430.
- [28] P. Geerlings, F. De Proft, W. Langenaeker, *Chem. Rev.* 103 (2003) 1793-1873.
- [29] P.K. Chattaraj, S. Giri, *J. Phys. Chem. A* 111 (2007) 11116-11121.
- [30] D. Kivelson, R. Niemen, *J. Chem. Phys.* 35 (1961) 149-155.
- [31] H. Irving, H. S. Rossotti, *J. Chem. Soc.* (1954) 2904-2910.
- [32] E. Farkas, H. Csoka, *J. Inorg. Biochem.* 89 (2002) 219-226.
- [33] M.M. Omar, G. G. Mohamed, *Spectrochim. Acta A* 61 (2005) 929-936.
- [34] H. Irving, H. S. Rossotti, *J. Chem. Soc.* (1953) 3397-3405.
- [35] F.J.C. Rossotti, H.S. Rossotti, *Acta Chem. Scand.* 9 (1955) 1166-1176.
- [36] M.T. Beck, I. Nagybal, *Chemistry of Complex Equilibrium*, Wiley, New York (1990).
- [37] M.M. Khalil, A.M. Radalla, A.G. Mohamed, *J. Chem. Eng. Data* 54 (2009) 3261-3272.
- [38] P. Sanyal, G.P. Sengupta, *J. Ind. Chem. Soc.* 67 (1990) 342-344.
- [39] S. Sridhar, P. Kulanthaipandi, P. Thillaiarasu, V. Thanikachalam, G. Manikandan, *J. Chem.* 4 (2009) 133-140.
- [40] V.D. Athawale, V. Lele, *J. Chem. Eng. Data* 41 (1996) 1015-1019.
- [41] V.D. Athawale, S.S. Nerkar, *Monatsh. Chem.* 131 (2000) 267-276.
- [42] G.A. Ibañez, G. M. Escandar, *Polyhedron* 17 (1998) 4433-4441.
- [43] W.U. Malik, G.D. Tuli, R.D. Madan, *Selected Topics in Inorganic Chemistry*, 3rd Edition. Chand, S. & Company LTD, New Delhi (1984).
- [44] G.C. Mohamed, M.M. Omar, A. Ibrahim, *Eur. J. Med. Chem.* 44 (2009) 4801-4812.
- [45] F.R. Harlly, R.M. Burgess, R.M. Alcock, *Solution Equilibria*, p. 257. Ellis Harwood, Chichester (1980).
- [46] L.E. Orgel, *An Introduction to Transition Metal Chemistry Ligand Field Theory*, p. 55. Methuen, London (1966).
- [47] K.D. Bhesaniya, S. Baluja, *J. Mol. Liq.* 190 (2014) 190-195.
- [48] A. Bebot-Bringaud, C. Dange, N. Fauconnier, C. Gerard, *J. Inorg. Biochem.* 75 (1999) 71-78.
- [49] A.A. El-Bindary, A.Z. El-Sonbati, M.A. Diab, M.K. Abd El-Kader, *J. Chemistry*, 2013 (2013) 1-6.